

# Experimental Analysis of Original and Strengthened Traditional Timber Connections

**Jorge Branco**  
PhD Student  
University of Minho  
Guimarães, Portugal

**Paulo Cruz**  
Associate Professor  
University of Minho  
Guimarães, Portugal

**Maurizio Piazza**  
Professor  
University of Trento  
Trento, Italy

**Humberto Varum**  
Assistant Professor  
University of Aveiro  
Aveiro, Portugal

## Summary

Tests on full-scale unstrengthened connections were performed under monotonic and cyclic loading. Attention has been principally focused on the birdsmouth joint, because of its common use in practice. Different strengthening solutions with metal elements have been evaluated.

## 1. Introduction

The most common joint in existing roof timber structures is the “birds-mouth joint with a single tooth”, although geometry varies with joint location in the truss, and the joint bearing capacity is function of skew angle, notch depth and length of the toe. The load transmission relies on direct contact and friction between facing surfaces. Metal ties or fasteners do not transmit forces directly; they were mainly used for positioning and to maintain the functionality of the joint in adverse or unpredictable conditions.

Common timber roof structures are usually modelled with perfect hinges at the ends of each element. However, these joints offer a significant moment resistance and may be better classified as semi-rigid. The lack of practical but realistic models for the joints in old traditional timber structures generally leads to very conservative retrofits and upgrades to satisfy new safety and serviceability requirements. Moreover, the misunderstanding of the global behaviour of traditional roof trusses can result in unacceptable stresses in the members as a result of inappropriate joints strengthening (in terms of stiffening).

Joints strengthening can be done in a number of possible ways: from simple replacement or addition of fasteners, to the use of metal plates, glued composites or even full injection with fluid adhesives. Each solution has unique consequences in terms of the joint final strength, stiffness and ductility. Although being widely used, the number of studies on the mechanical performance of existing traditional carpentry joints and possible strengthening techniques is not worldwide. With few exceptions (e.g. King et al. 1999 [1]; Bulleit et al. 1999 [2]; Seo et al. 1999 [3] and Parisi et al. 2000 [4]), timber joints research has been oriented towards new engineered configurations.

A research program has been developed by the authors with the purpose of investigating the monotonic and cyclic behaviours of old timber connections and identifying and evaluating suitable strengthening techniques. This research addresses both unstrengthened and strengthened connections under monotonic and cyclic loading.

Test data of original connections have been gathered with the purpose of characterizing their behaviour as well as to allow the calibration of numerical models. The tested specimens could not cover all the possible ranges and combination of parameters (as geometry, compression level, loading test velocity, etc.) that are of practical interest. The experimental analysis can be extended by numerical models in the next research step. Beyond this, experimentation gave an insight of the joint behaviour for the calibration of the models. It was particularly important to observe the post-elastic behaviour and the failure mode of the connections. Observing the behaviour of strengthened connections under cyclic loading gave straight indications on the positive and negative characteristics of the different strengthening techniques that have been analysed.

## 2. Experimental campaign

The experimental research was carried out at the Laboratory of Structures of the University of Minho (Portugal), and includes monotonic and cyclic tests of full-scale birdsmouth joints [5].

Table 1 Tests on birdsmouth joints

Connection		Number of Specimens	Loading Method	$\sigma_c$ (MPa)
Unstrengthened (original)		3	Mono. +	1.4
		3	Mono. -	1.4
		3	Cyclic	1.4
		3	Mono. +	2.5
		3	Mono. -	2.5
		3	Cyclic	2.5
Strengthened	Stirrup	3	Mono. +	1.4
		3	Mono. -	1.4
		3	Cyclic	1.4
	Bolt	3	Mono. +	1.4
		3	Mono. -	1.4
		3	Cyclic	1.4
	Binding Strip	3	Mono. +	1.4
		3	Mono. -	1.4
		3	Cyclic	1.4

Note:  $\sigma_c$  is the rafter compression stress level

A series of tests on unstrengthened specimens were performed in order to characterize the original behaviour of joints representative of existing timber systems. Subsequently, a set of joints were strengthened with metal devices and tested under monotonic and cyclic loading. Tests on assembled connections were preceded by accurate material characterization, in terms of the mechanical properties of the timber elements used for all full-scale models. Table 1 summarises the test campaign conducted on birdsmouth joints.

## 2.1 Material properties

A mechanical characterization of the timber used in the joints (*Pinus Pinaster* Ait.) was performed. In the carpentry where the joints were fabricated, all timber pieces used were classified as belonging to quality class EE as result of a visual strength grading according the Portuguese National Standard NP 4305:1995 [6]. At the laboratory, over some samples collected during the fabrication of the joints, the local and global Young's modulus and strength, both in bending and compression parallel to the grain, were estimated following the prEN408:2000 [7].

## 2.2 Test setup and instrumentation

A steel test-hand able to accommodate specimens with various skew angles was built within a larger steel loading frame of the laboratory (Figure 1). The arrangement allows independent control of two hydraulic jacks. One jack, aligned with the rafter, induced constant compression throughout the test. The other, a double-acting jack, positioned at a height of 70 cm above the center of the joint, apply a transversal force, with a programmed load cycle, and generated a moment at the joint. Force ( $F$ ) versus displacement ( $d$ ) curves were measured. The two jacks have a maximum loading capacity of 50 kN and 100 kN and a maximum stroke of 160 mm and 50 mm, respectively. Type and location of instrumental channels, including load cells and linear voltage differential transducers (LVDT), are shown in Figure 1.

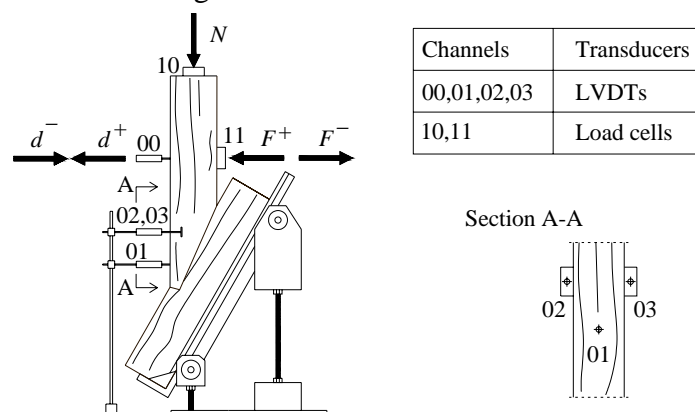


Fig 1 Testing apparatus and instrumentation layout

Tests were performed under displacement control for the typical birdsmouth joint skew angle of  $30^\circ$ . For all the specimens, the cross sections of the elements were  $80 \times 220 \text{ mm}^2$ , the notch depth was 45 mm and the notch length was 422 mm as represented in Figure 2.

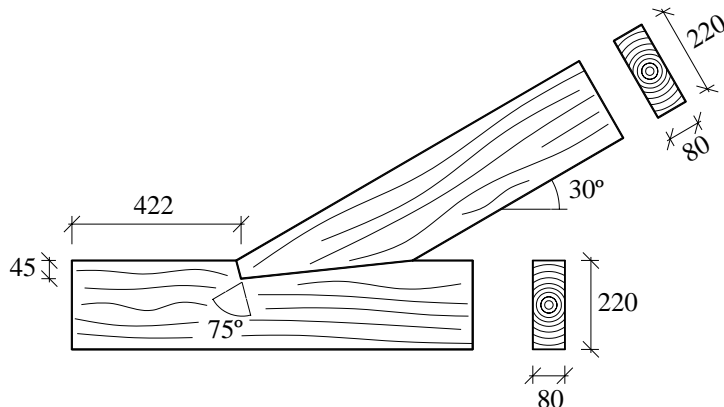


Fig 2 Connections geometry (dimensions in millimetres)

The first step of the loading procedures in both the monotonic and cyclic tests was the application of an axial compression force on the rafter. This force, simulating the effect of the self-weight and dead load presented in the structure, was kept constant during the test. In the subsequent loading steps, a transversal force,  $F$ , acts perpendicular to the rafter axis. When the skew angle increases, it is defined as the positive direction and when the skew angle decreases, it is defined as the

negative direction. Monotonic tests were performed to determine the elastic behaviour, in particular, the apparent elastic limit displacement  $d_e^+$  and  $d_e^-$ . Under displacement control at channel 00, a maximum displacement value of 50 mm, was imposed under a velocity of 0.028 mm/s.

### 2.3 Cyclic test procedures

Full-scale connections, similar to the specimens of monotonic loading were tested with a quasi-static cyclic loading. In particular, the test program included one cycle in the range  $[0.25 d_e^+; 0.25 d_e^-]$ ; one cycle in the range  $[0.50 d_e^+; 0.50 d_e^-]$ ; three cycles in the range  $[0.75 d_e^+; 0.75 d_e^-]$ ; three cycles in the range  $[(1+n) d_e^+; (1+n) d_e^-]$  with  $n = 0, 1, 2, \dots$  until joints failure. This sequence is in accordance with the proposal in reference [8]. The values used for the elastic limit displacements, for both positive ( $d_e^+$ ) and negative ( $d_e^-$ ) directions, came directly from the results achieved in the monotonic tests.

### 2.4 Strengthening solutions studied

Metal connectors have been applied occasionally in timber joints since very ancient times. Although this practice became common only in the 19<sup>th</sup> century, when the development of industrial production methods made bolts, rivets, and other metal elements easily available. Metal devices were intended to counteract out-of-plane actions, which could not be resisted by the assemblage itself. Nowadays, strengthening also concerns the behaviour of the friction-based connection in its own plane, and is intended to avoid the detachment of the connected members. Particularly in seismic areas, strengthening can prevent loss of capacity and possible separation of friction surfaces due to the decrease of compression forces, and, under cyclic loading, the application of strengthened solutions can maintain a stable behaviour [4]. The three basic types of intervention considered in this study are modern implementations of traditional strengthening techniques: the stirrups, the internal bolt and the binding strip (Figure 3).

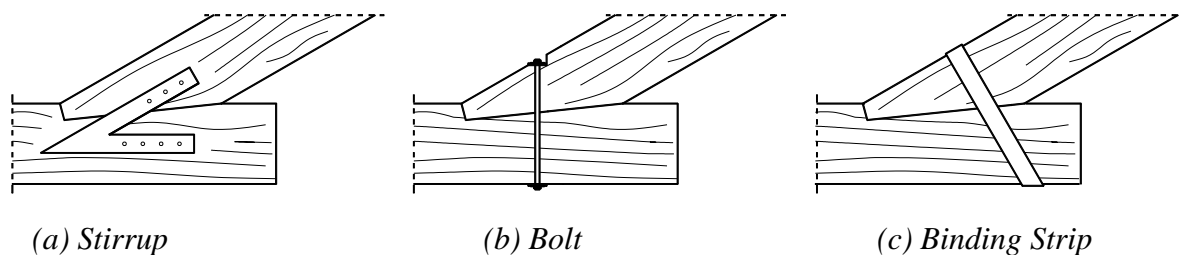


Fig 3 Traditional strengthening techniques evaluated

Metal stirrups placed in pairs at two opposite sides of the joint were very popular in the past and are still considered adequate and frequently adopted. The effect of the large increase of in-plane

stiffness connection is particularly important and should be investigated. In this study, each stirrup was composed of two steel plates welded in a V-shape. Each prong was 50 mm wide and 5 mm thick. They were parallel to the rafter or to the chord, and bolted to it with seven bolts of 10 mm diameter. The use of a steel rod, with 12 mm diameter, was also considered. The rod was fixed by a nut at both ends and secured using a special rectangular-shape washer (70 x 30 mm<sup>2</sup> and 5 mm thick). A suitable seat area was formed within the timber element for accommodating it, which allows perfect contact between surfaces. The rod was located at the midjoint and normal to the axis of the rafter. Metal binding strips, considered obsolete today, were very frequently adopted in the 19<sup>th</sup> century roof structures, particularly to strengthen the lower rafter and chord connections in configurations having skew angles typically of 30° [9]. An updated version of this layout was considered here: the joint was bound with a hollow steel ribbon, 50 mm wide and 5 mm thick, located at midjoint, normal to the chord.

### 3. Test results

#### 3.1 Evaluation of the original unstrengthened connections

The first set of connections tested was composed by three unstrengthened joints (A1, A2 and A3). A permanent compression force of 25 kN (corresponding to 1.4 MPa compression stress) was applied to the rafter throughout the vertical jack, and the second jack imposed a monotonic transversal force (perpendicular to rafter axis). The test results illustrate perfect elasto-plastic behaviour for the three curves (Figure 4). The behaviour is perfectly elastic until the elastic limit displacement ( $\approx 8$  mm), after which became non-linear but only within a small range. Subsequently, a quasi-perfect plastic behaviour appears. This pseudo-plastic phase, starting at a 10 mm displacement, remains practically constant until the maximum displacement (50 mm), presenting a small decrease of the resistance after 25 mm displacement.

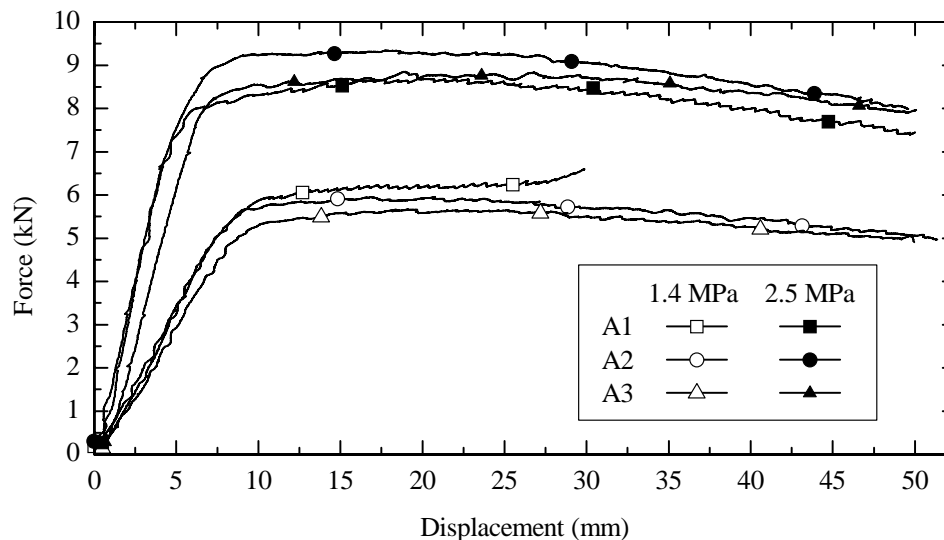


*Fig 4 Force-displacement curves obtained in the positive direction for different rafter compression stress level*

A more brittle behaviour was detected when the skew angle decreases. The curves presented in Figure 5 shows a behaviour perfectly elastic just at the maximum force, after which a slip, followed by a loss of friction, induces a rapid decrease of the resistance. After the new stable position of the joint is reached, the brittle behaviour is substituted by a pseudo-plastic phase. This ductile behaviour is due to the local compression of wood. Finally, a total loss of friction occurs with the failure of the connection. The subsequent sets of tests aim to evaluate the influence of the compression stress level applied in the rafter. The two first sets were analysed under a compression level of 25 kN, corresponding to a compression stress of 1.4 MPa, representing the dead load applied on the roof structure. Later, a compression force of 44 kN, corresponding to a stress level of 2.5 MPa, was used.

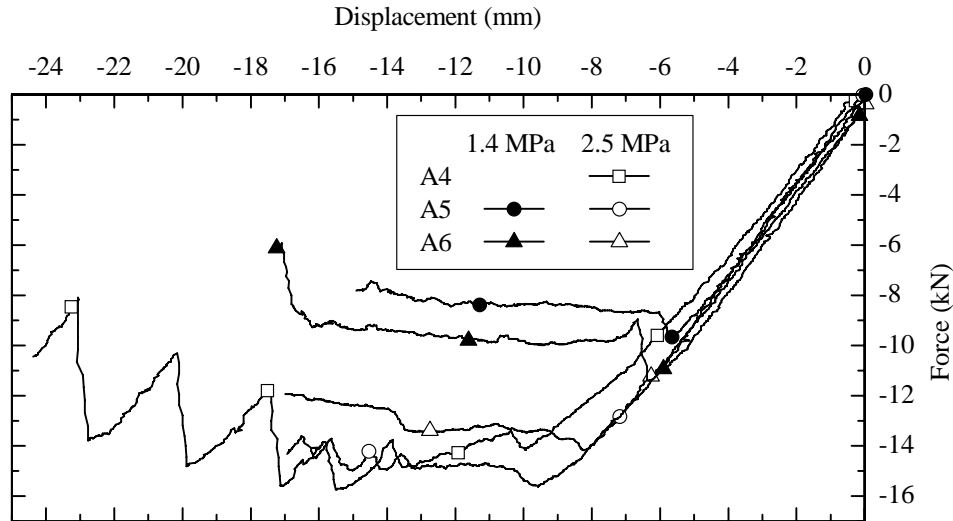


Fig 5 Force-displacement curves obtained in the negative field for different rafter compression stress level

The stress level adopted in these tests was defined for the serviceability limits states defined according standards for common Portuguese timber roof structures [9]. Comparing the force-displacement curves obtained from the two different compression levels, with the decrease of the skew angle (negative direction), only an increasing in the maximum force and corresponding elastic limit displacement can be observed. The same brittle behaviour after the achievement of the elastic displacement limit is observed. The curves, for what concerns the initial stiffness characteristics, remain nearly constant. In the other direction, the positive field, apart of an increasing in the maximum force, a higher initial stiffness is also achieved with the increase of the compression stress level in the rafter (Figure 4). However, the shapes of the curves are similar. Table 2 summarises the main results for the monotonic tests conducted for the different compression stress levels.

Table 2 Influence of the compression stress level in the rafter in the response for monotonic loading

$\sigma_c$ (MPa)	$d_e^+$ (mm)	$d_e^-$ (mm)	$F_{max}$ (kN)	Stiffness (kN/mm) x $10^3$		
				Regression	$F_e / d_e$	$F_e^{50\%} / d_e^{50\%}$
1.4	8.31	–	6.72	674	634	647
	–	5.76	-10.75	1771	1785	1958
2.5	5.47	–	10.84	1569	1389	1408
	–	8.13	-15.32	1705	1661	1758

Figure 6 shows the effect of the compression stress level in the rafter under cyclic loading for the specimen A9. The obtained response is not symmetric. Energy dissipation occurs only in the negative direction. On the contrary, the positive direction does not present any dissipation of energy. But the force-displacement curves show a non-linear development in both directions. This energy dissipation is mainly produced by the sliding of the rafter when pulled into the negative direction. Increasing the compression stress level at the rafter, the force-displacement curves remain similar, presenting an increment in the maximum force values. The energy dissipation grows with the compression stress level in the rafter (2.5% to 3.96% in the hysteretic equivalent viscous damping ratio,  $V_{eq}$ ). The main difference between the compression stress levels applied in the rafter was that, for 1.4 MPa, no failure was reached, while, with 2.5 MPa, all three specimens collapsed.

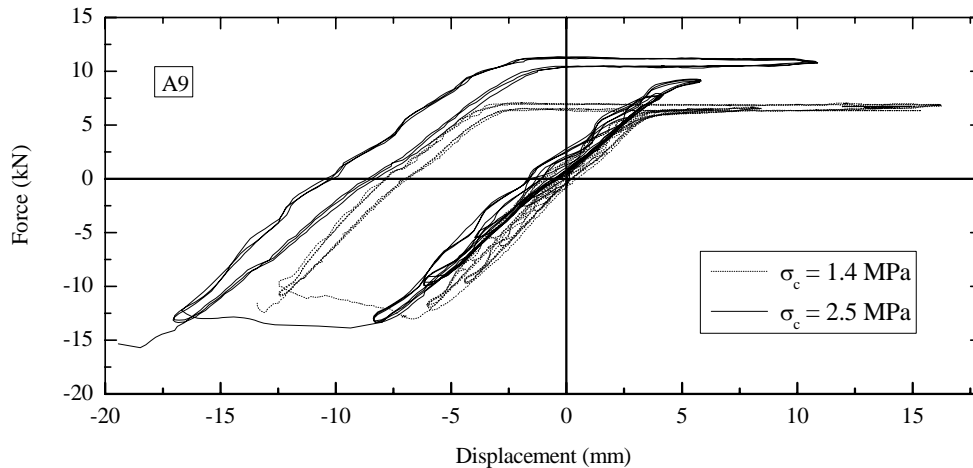
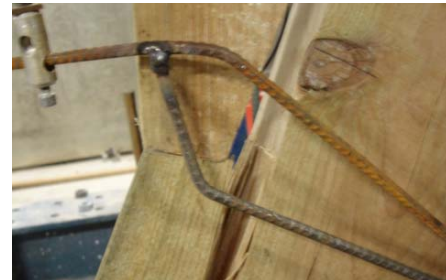


*Fig 6 Influence of the rafter compression stress level in the cyclic tests*

In Figure 7, the failure modes show compression damages in the joints and the development of a shear failure surface in front of the joint itself.



*(a) Compression damage in A7*



*(b) Shear failure in A9*

*Fig 7 Damages in the joints observed in the cyclic tests for 2.5 MPa rafter compression stress level*

### **3.2 Efficiency evaluation of the strengthening techniques**

Comparing the tests results in terms of force-displacement curves for the unstrengthened and strengthened connections (Figure 8), it is recognized that all the strengthening schemes analysed increase the stiffness, in particular, in the positive direction and the maximum resistance for both directions. The elasto-plastic behaviour with limited ductility evidenced by the unstrengthened connections is substituted by full non-linear curves exhibiting high ductility in the strengthened connections. Comparing the strengthening techniques evaluated, the less efficient, in terms of maximum resistance, is the internal bolt, while the elastic stiffness are similar. Connections strengthened with stirrups and binding strip attained the same range of maximum force, however, this last scheme has a lower ductility capacity. In particular, the maximum resistance for the strengthened connections with stirrups and internal bolt is achieved near the end of the test. However, in the strengthened connections with binding strip, when the tests were interrupted, the force value was already decreased. Therefore, between the internal bolt and the binding strip, the first one is more efficient in terms of ductility capacity with the goal to assure a better seismic behaviour of the joints. The effect of the strengthening schemes in the negative directions of the monotonic tests is quite obvious: the maximum resistance and the ductility capacity increase. The benefits in terms of stiffness are not so significant. However, the brittle behaviour exhibited by unstrengthened connections disappears in the strengthened specimens. Therefore, the main profit of adding a metal device to the joints is the improvement of ductility with clear advantages in their seismic behaviour. Only the binding strip showed limitations in terms of maximum displacement.

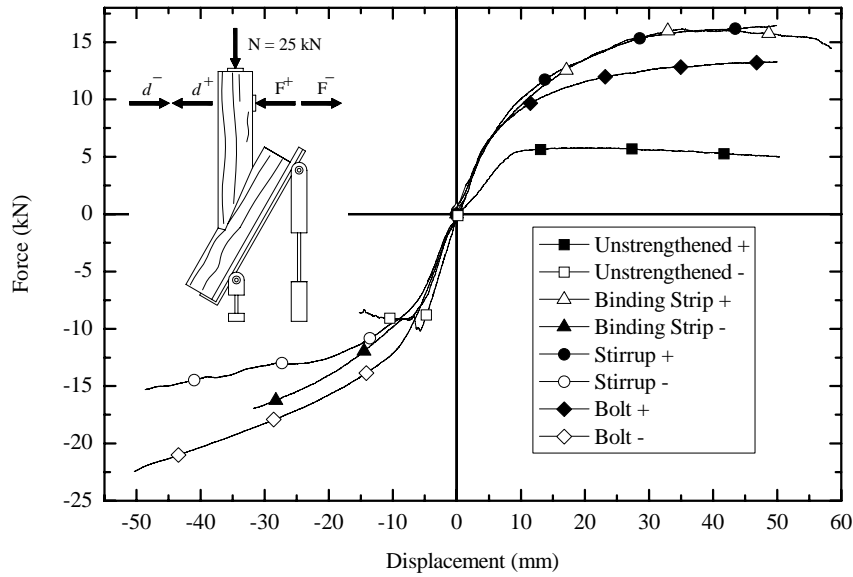


Fig 8 Force-displacement diagrams for unstrengthened and strengthened connections under monotonic loading

Figure 9 shows the common failure modes and principal damages detected in the cyclic tests on the strengthened connections. Table 3 summarises the main results of the cyclic tests on the strengthened joints.



(a) Compression in the joint with the binding strip



(b) Bending of the bolt with local embedment



(c) Stirrup failure

Fig 9 Failure modes and damages detected during the cyclic tests on the strengthened connections

Table 3 Main results for the cyclic tests on the original and strengthened joints (average values)

Joint	Dissipated Energy (kJ)	Ve <sub>q</sub> (%)	$d_{max}^+$ (mm)	$d_{max}^-$ (mm)	$F_{max}^+$ (kN)	$F_{max}^-$ (kN)
Unstrengthened ( $\sigma_c=1.4$ MPa)	230	2.45	16.49	-15.83	6.20	-11.57
Unstrengthened ( $\sigma_c=2.5$ MPa)	380	3.96	9.15	-21.17	9.45	-17.00
Binding Strip	2874	6.85	18.38	-39.63	23.38	-25.47
Bolt	1877	11.28	13.30	-35.30	15.29	-21.08
Stirrup	1859	14.57	28.68	-21.75	18.09	-15.60

As it was already pointed out, the behaviour of the joints depends largely on the rafter compression stress level. All strengthening techniques adopted were efficient in the improvement of the hysteretic behaviour of the connections. Hysteretic equivalent viscous damping ratios ( $Ve_q$ ) evaluated from test results are considerable. With more cycles achieved, more energy is dissipated. Figure 10 collects the force-displacement diagrams for cyclic loading on the strengthened and original unstrengthened joints with a rafter compression stress level of 1.4 MPa.

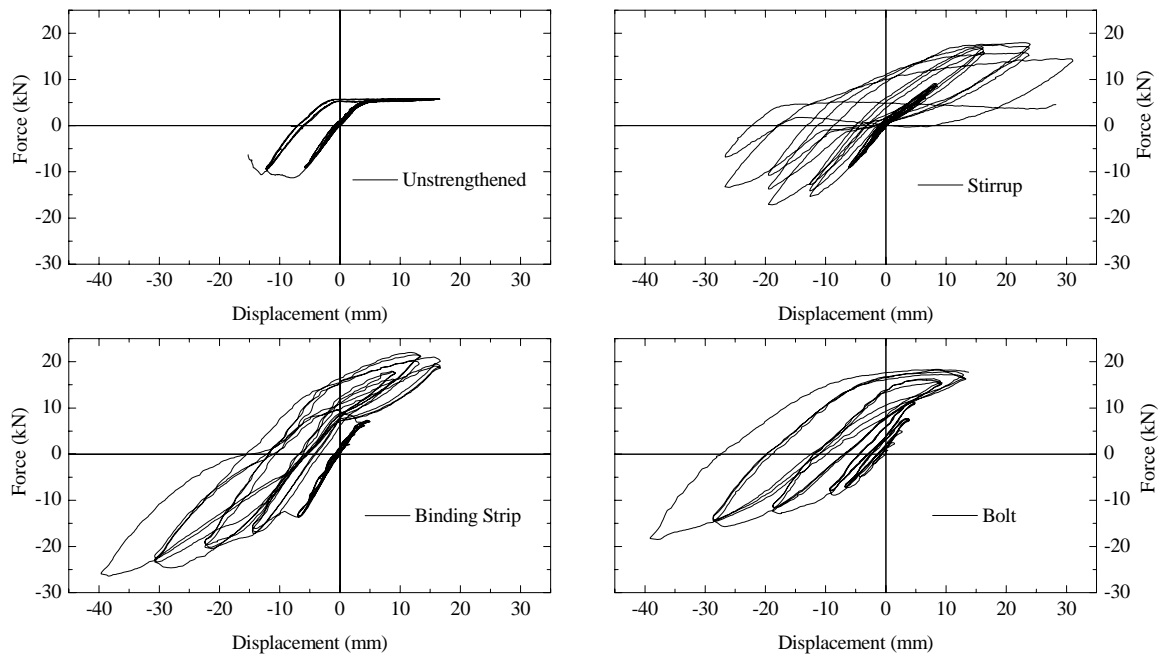


Fig 10 Force-displacement response for the cyclic loading (rafter compression level of 1.4 MPa)

#### 4. Main conclusions and final considerations

The birdsmouth joint, even without any strengthening device, has a significant moment-resisting capacity. The test results show that this capacity is function of the rafter compression stress level. However, it is clear that the width of the rafter, the friction angle, and the skew angle in the connection are also important. The experimental analysis has been of fundamental importance in order to understand the real behaviour, pointing out some important aspects like force transmission mechanism, failure modes and guidance for appropriate strengthening solutions. Strengthening, usually performed by insertion of metal devices, is indispensable for ensuring adequate joint response, in particular, in seismic regions, or in adverse and unpredictable loading conditions. The joint strengthening results in a significant increase of the hysteretic equivalent viscous damping ratio ( $V_{eq}$ ). The energy dissipation became significantly higher. Therefore, the strengthening solutions studied improve the seismic behaviour of the birdsmouth joints typically presented in traditional timber roofs.

#### 5. References

- [1] Bulleit W. M., Sandberg B. L., Drewek M. W., and O'Bryant T. L. 1999. Behaviour and modelling of wood-pegged timber frames. *J.Struct. Engrg.*, ASCE, 125(1), 3–9.
- [2] King W. S., Yen R. J. Y., and Yen A. Y. N. 1996. Joint characteristics of traditional Chinese wooden frames. *Engrg. Struct.*, 18(8), 635–644.
- [3] Seo J.-M., Choi I.-K., and Lee J.-R. 1999. Static and cyclic behaviour of wooden frames with tenon joints under lateral load. *J. Struct. Engrg.*, ASCE, 125(3), 344–349.
- [4] Parisi M. A, and Piazza M. 2000. Mechanics of plain and retrofitted traditional timber connections. *J Struct Engrg.*, ASCE; 126(12): 1395–403.
- [5] Branco J., Cruz P., and Varum H. 2005. *Experimental Analysis of Birdsmouth Joints*. Report E-11/05. DECivil, University of Minho, 49 pp.
- [6] NP 4305:1995. *Structural maritime pine swan timber – Visual grading*, CT 14 LNEC.
- [7] prEN 408:2000. *Timber structures – Structural timber and glued laminated timber – Determination of some physical and mechanical properties*. CEN.
- [8] Dolan J. D. 1994. RILEM Technical Committee 109 TSA, Timber Structures in Seismic Regions, *Materials and Structures*, Vol. 27, 167, pp. 157-184.
- [9] Branco J., Cruz P., Varum H., and Piazza M. 2005. *Portuguese traditional timber trusses: static and dynamic behaviour*. Report E-19/05. DECivil, University of Minho, 50 pp.